COMMUNICATIONS

Three-Component Reactions

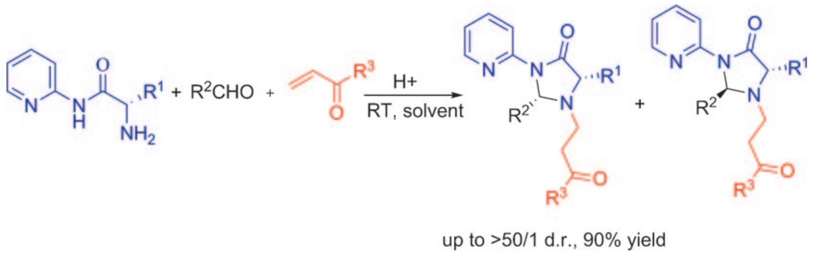

In control: An α-amino amide reacted with an aldehyde and a Michael acceptor to form stable imidazolidin-4-ones with high stereoselectivity. A dynamic kinetic aza-Michael addition was discovered and applied to the three-component reaction to enforce high stereoselectivity. A remote group was incorporated to invert the reaction process and direct the reaction towards the desired product (see scheme).

Quinone Synthesis

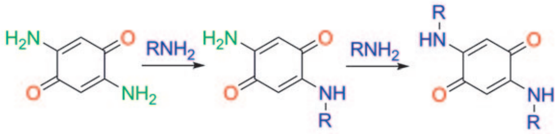

Keep it simple: A new transamination method is reported for the synthesis of diamino-substituted *p*-quinones (see scheme). Asymmetrically substituted *p*-quinones are shown to be key intermediates in this reaction. The redox properties of these ligands are discussed and their utility in coordination and redox chemistry is shown with a representative example.

Coordination Polymers

The right to choose: 1,2,4-Diazaphospholide anions support the predictable construction of coordination polymer networks of different topology by switching between bidentate (κ*N*,κ*N*′) and tridentate (κ*N*,κ*N*′,κ*P*) coordination depending on the choice of the metal (see picture); furthermore, the ligand exhibits a remarkable difference to 1,2,4-triazolides because the diffuse lone pair at phosphorus permits μ_2(P)-bridging coordination.

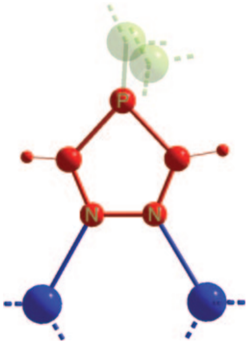

Antibiotics

Sugar sugar! The synthesis and evaluation of ribostamycin/kanamycin hybrids incorporating a highly crowded trisubstituted aminocyclitol unit that should provide maximum complementation with the RNA receptor are reported (see picture). Analysis shows that the existing conflicts between the different sugar rings can be significantly alleviated by a simple chemical modification, leading to an improvement in activity.

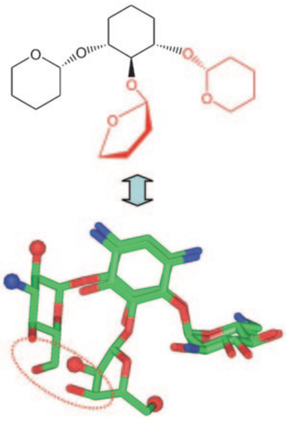

pH Sensors

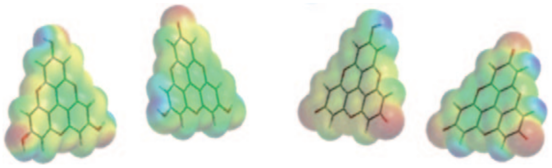

Fluorescein ver. 2.0: A new, highly fluorescent, pH-sensitive trihydroxytrioxatriangulenium dye (H-TOTA) has been synthesised and characterised. The dye is closely related to fluorescein and may be considered to be a two-dimensional extended version. This new dye can exist in four different protonation states (see graphic) depending on the pH, and its use as a sensitive fluorescent ratiometric pH probe in a physiological buffer is demonstrated.

Molecular Switches

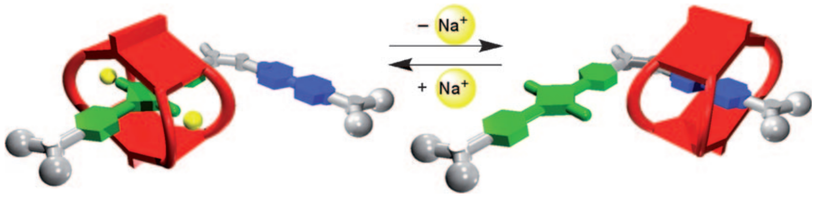

In a flash! A squaraine-based optical molecular switch functions with striking fluorescence signal changes that are visible to the naked eye (see figure).

Vesicles

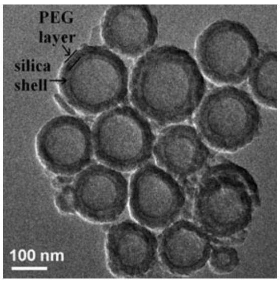

Delivery by stealth: Vesicles with porous silica shell layers and poly(ethylene glycol) (PEG) stealth layers have good stability, due to the silica layers, good dispersity in aqueous solution, without aggregation due to the PEG stealth layers, low cytotoxicity, and the capability to enter cells (see figure).

Heterocycles

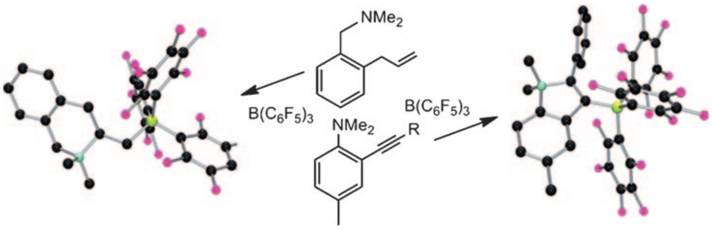

Intramolecular additions of amines to olefinic and acetylenic residues in the presence of $B(C_6F_5)_3$ affords a "frustrated Lewis Pair" strategy to five- and six-membered-ring heterocyclic ammonium borate derivatives (see picture).

Frontiers of Chemistry:
From Molecules to Systems

A One-Day Symposium

Celebrating 10 Years of

On 21st May 2010 in Paris

at the Maison de la Chimie
(near the Eiffel Tower and Les Invalides)

Speakers


Gerhard Ertl
Nobel Prize 2007


Jean-Marie Lehn
Nobel Prize 1987


Roger Y. Tsien
Nobel Prize 2008


Ada Yonath
Nobel Prize 2009


Luisa De Cola


Alan R. Fersht


Marc Fontecave


Michael Grätzel


Michel Orrit


Nicolas Winssinger

Scientific committee

E. Amouyal, M. Che,
F. C. De Schryver,
A. R. Fersht, P. Gölitz,
J. T. Hynes, J.-M. Lehn

Posters

will be displayed also online from 1st April

www.chembiophyschem.org

Topics

catalysis, biochemical imaging, chemical biology, bionanotechnology, proteomics, spectroscopy, solar cells

Organized by

ChemPubSoc Europe

Société Chimique de France

Partner of the event sanofi aventis
Because health matters

WILEY-VCH

557101001

Macrocycles

J. Song, P. Kim, N. Aratani, D. Kim, H. Shinokubo,* A. Osuka** 3009 – 3012

Strategic Synthesis of 2,6-Pyridylene-Bridged β-to-β Porphyrin Nanorings through Cross-Coupling

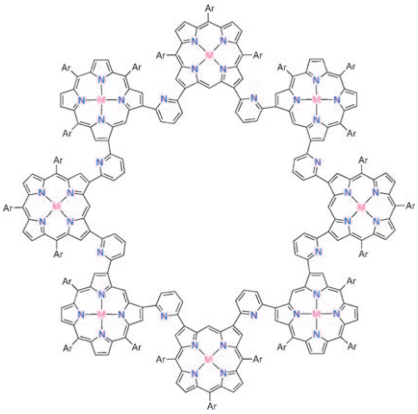

The bridge determines the size of the loop? Palladium-catalyzed cross-coupling of borylporphyrins led to the construction of β-pyridine-bridged porphyrin nanorings in good yields (around 55–60 %; see scheme). The photophysical study revealed that these nanorings exhibit weakly coupled chromophores and longer fluorescent lifetimes, which is an apparent advantage in the process of efficient excited energy transfer.

FULL PAPERS

Disilamolybdenocenophane

T. Arnold, H. Braunschweig, M. Gross, M. Kaupp,* R. Müller, K. Radacki* .... 3014 – 3020

Electronic Structure and Reactivity of a [1],[1]Disilamolybdenocenophane

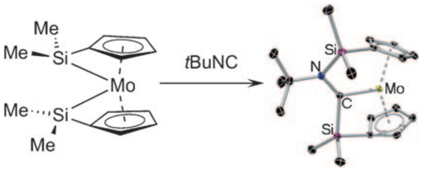

A surprising *ansa*! The electronic structure of [1],[1]disilamolybdenocenophane has been analyzed by means of DFT. As predicted from the metal-based nucleophilicity and strained geometry, remarkable reactivity towards nonpolar and polar unsaturated organic substrates has been observed. For instance, treatment with *tert*-butylisonitrile leads to a highly unusual structural motif, an *ansa*-carbene (see scheme).

Asymmetric Organocatalysis

S. Xu, Z. Wang, Y. Li, X. Zhang, H. Wang, K. Ding** .... 3021 – 3035

Mechanistic Investigation of Chiral Phosphoric Acid Catalyzed Asymmetric Baeyer–Villiger Reaction of 3-Substituted Cyclobutanones with H_2O_2 as the Oxidant

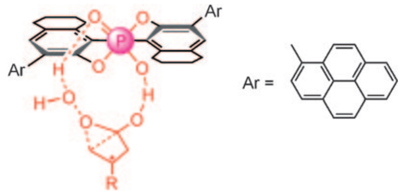

Bifunctional catalysis: Excellent agreement between experimental observations and theoretical calculations was found in the understanding of the mechanism of the chiral phosphoric acid catalyzed asymmetric Baeyer–Villiger reaction of cyclobutanones with H_2O_2 as the oxidant. The transition state for the reaction is depicted.

DNA Recognition

L. Hernandez-Folgado, D. Baretić, I. Piantanida, M. Marjanović, M. Kralj, T. Rehm, C. Schmuck** .... 3036 – 3056

Guanidiniocarbonylpyrrole–Aryl Derivatives: Structure Tuning for Spectrophotometric Recognition of Specific DNA and RNA Sequences and for Antiproliferative Activity

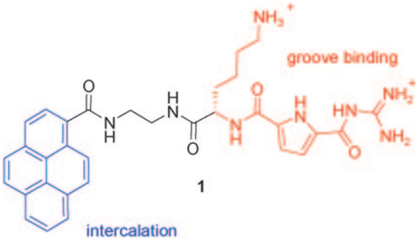

DNA sensors: A systematic study of guanidiniocarbonylpyrrole–aryl derivatives designed to interact with DNA or RNA both through intercalation and through groove binding is presented. Distinctively different interactions with either DNA or RNA are seen by UV/Vis, fluorescence and CD spectroscopy. Compound **1** (see graphic), for example, shows base-pair-selective recognition of ds-DNA.

Base Pairing

J. E. Šponer, Á. Vázquez-Mayagoitia,*
B. G. Sumpter, J. Leszczynski,
J. Šponer, M. Otyepka, P. Banáš,*
*M. Fuentes-Cabrera** 3057–3065

Theoretical Studies on the Intermolecular Interactions of Potentially Primordial Base-Pair Analogues

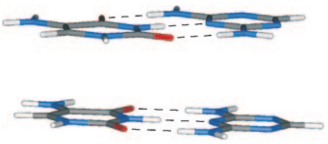

Melting temperature versus pK_a: Quantum chemical calculations on the Watson–Crick-type base pairing and stacking properties of triazine- and aminopyrimidine-based primordial informational oligomers (see graphic) show that neither the intrinsic base pairing nor the stacking interactions are responsible for the experimentally observed relationship between the pK_a values of the participating heterocycles and the melting points of the duplexes.

Organic gelators

V. Čaplar, L. Frkanec, N. Š. Vujičić,
*M. Žinić** 3066–3082

Positionally Isomeric Organic Gelators: Structure–Gelation Study, Racemic versus Enantiomeric Gelators, and Solvation Effects

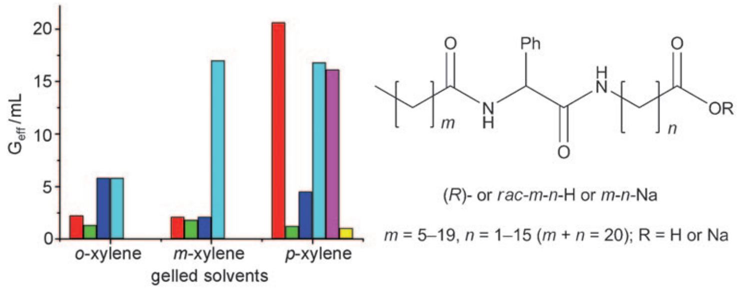

Positionally isomeric gelators: Members of a series of positionally isomeric gelators based on long alkyl chains, a hydrogen-bonding phenylglycine unit, and a terminal carboxylic acid or sodium carboxylate moiety (see figure) have been found to display significantly different gelation properties. Dramatic differences in gelator effectiveness (G_{eff}) values of up to 70 times could be observed between racemate/enantiomer gelator pairs, an effect that was observable even in the gelation of very similar solvents such as isomeric xylenes.

Biomimetics

T. Liu, B. Li, C. V. Popescu, A. Bilko,*
*L. M. Pérez, M. B. Hall,**
*M. Y. Darensbourg** 3083–3089

Analysis of a Pentacoordinate Iron Dicarbonyl as Synthetic Analogue of the Hmd or Mono-Iron Hydrogenase Active Site

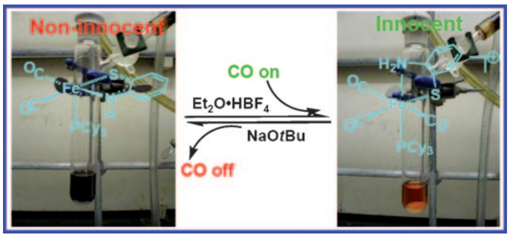

Salvation for the guilty: Protonation of a π-delocalizing, non-innocent ligand complex of iron developed as a pentacoordinate, dicarbonyl analogue of the [Fe]-H_2ase or Hmd (H_2-forming methylene-tetrahydromethanopterin dehydrogenase) enzyme active site, decreases the electron density at iron and engenders CO uptake as expected for d^6 Fe^{II} and as seen in the [Fe]-H_2ase enzyme active site. Deprotonation releases the extrinsic CO and reclaims the pentacoordinate iron in a state of electrophilic deficiency (see picture).

Asymmetric Catalysis

*T. Inagaki, L. T. Phong, A. Furuta, J.-i. Ito, H. Nishiyama** 3090–3096

Iron- and Cobalt-Catalyzed Asymmetric Hydrosilylation of Ketones and Enones with Bis(oxazolinylphenyl)amine Ligands

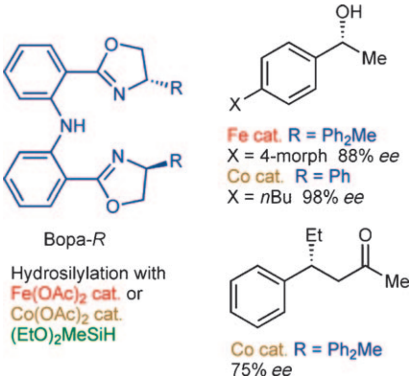

Chiral bis(oxazolinylphenyl)amines (Bopa-*R*) proved to be efficient auxiliary ligands for iron and cobalt catalysts that exhibit high activity for asymmetric hydrosilylation of ketones and asymmetric conjugate hydrosilylation of enones to give products such as those shown in the picture (4-morph = morpholino).

Antitumor Agents

*R. W.-Y. Sun, C. K.-L. Li, D.-L. Ma, J. J. Yan, C.-N. Lok, C.-H. Leung, N. Zhu, C.-M. Che** 3097–3113

Stable Anticancer Gold(III)–Porphyrin Complexes: Effects of Porphyrin Structure

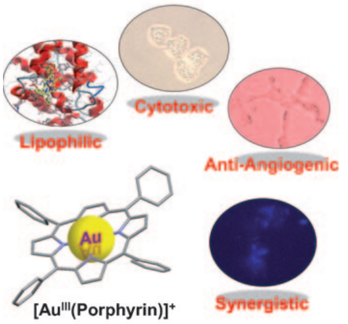

Fantastic gold! A family of stable lipophilic cations of the type $[Au^{III}(Por)]^+$ (Por = porphyrinato ligand) display promising in vitro cytotoxic and anti-angiogenic activities, and a synergistic property in cytotoxicity upon co-incubation with the fluorescent dye 4′,6-diamidino-2-phenylindole (DAPI, see graphic).

Ionic Liquids

*Y. Zhang, H. Gao, Y. Guo, Y.-H. Joo, J. M. Shreeve** 3114–3120

Hypergolic *N*,*N*-Dimethylhydrazinium Ionic Liquids

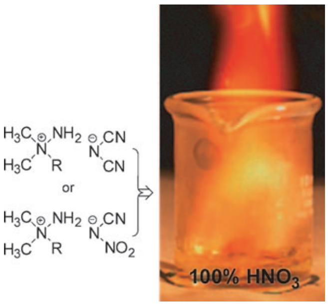

Fueling the fire: *N*-Alkyl-*N*,*N*-dimethylhydrazinium dicyanamide and nitrocyanamide ionic liquids are hypergolic with white-fuming nitric acid (see graphic). With extremely low vapor pressure, and high thermal and chemical stability, they should be less toxic than hydrazine and its derivatives, and have potential as liquid hypergolic fuels.

Photochemistry

D.-S. Hsu, Y.-Y. Chou, Y.-S. Tung, C.-C. Liao** 3121–3131

Photochemistry of Tricyclo[5.2.2.0^{2,6}]undeca-4,10-dien-8-ones: An Efficient General Route to Substituted Linear Triquinanes from 2-Methoxyphenols. Total Synthesis of (±)-Δ$^{9(12)}$-Capnellene

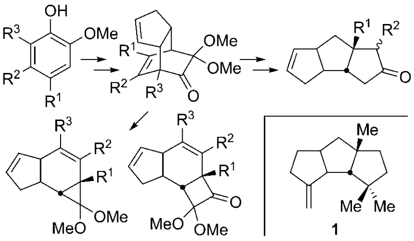

See the light! Photochemical reactions of a series of tricyclo[5.2.2.0^{2,6}]undeca-4,10-dien-8-ones were studied (see scheme). The oxa-di-π-methane rearranged products were further converted to linear triquinanes. This methodology was successfully applied to the total synthesis of (±)-Δ$^{9(12)}$-capnellene (**1**).

Nanospheres

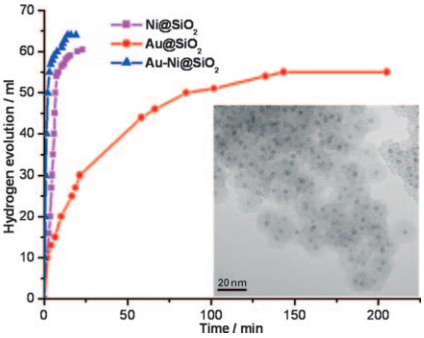

Bimetallic Au–Ni synergy: Bimetallic gold–nickel nanoparticles (NPs) with diameters of 3–4 nm embedded in silica nanospheres of around 15 nm have been prepared by a reversed-micelle technique and by in situ reduction in an aqueous $NaBH_4/NH_3BH_3$ solution. The combination of gold and nickel leads to a remarkable synergy not only in terms of catalytic activity (see figure), but also in durability in the hydrolysis of ammonia borane.

Encapsulation in Nanostructures

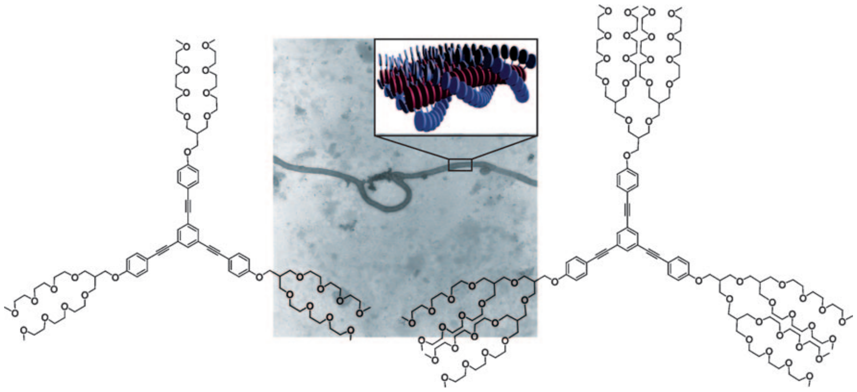

Shown the ropes! The rotated π stacking of dendronized oligo(phenylene ethynylene)s (see figure) results in the formation of nanofibrillar structures several micrometers long that can interact by the hydrophilic triethyleneglycol chains to form thicker strands. These supramolecular structures are able to intercalate and release dye molecules.

Reaction Mechanisms

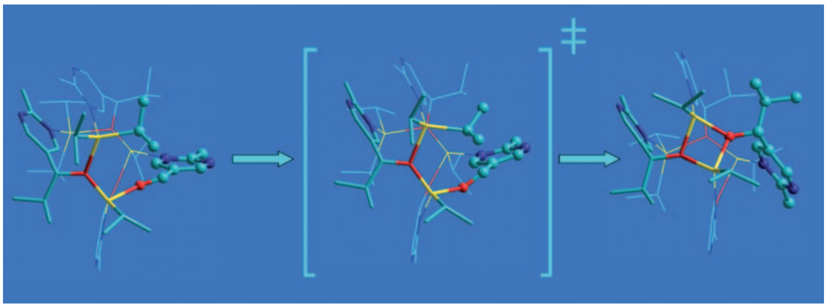

Interplay of three catalytic cycles explains the main features of the Soai reaction (see picture). These are the fully enantioselective catalytic cycle of the homochiral dimers (the dominant one), the catalytic cycle of the heterochiral dimer (in fact ineffective, as required for the Soai reaction to manifest chiral amplification), and the nonenantioselective catalytic cycle of the homochiral dimers (necessary to explain the observed enantioselectivity).

Ligand Design

Q.-X. Zhou, W.-H. Lei, J.-R. Chen, C. Li, Y.-J. Hou, X.-S. Wang, B.-W. Zhang** .... 3157 – 3165

A New Heteroleptic Ruthenium(II) Polypyridyl Complex with Long-Wavelength Absorption and High Singlet-Oxygen Quantum Yield

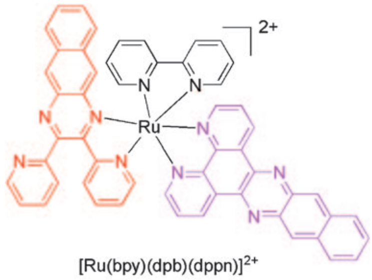

$[Ru(bpy)(dpb)(dppn)]^{2+}$

Effective cooperation of the ligands 2,3-bis(2-pyridyl)benzoquinoxaline (dpb) and 4,5,9,16-tetraaza-dibenzo-[*a*,*c*]naphthacene (dppn) gives the tris-heteroleptic complex $[Ru(bpy)(dpb)(dppn)]^{2+}$ (bpy = 2,2′-bipyridine), which has a metal-to-ligand charge-transfer maximum at 548 nm, a singlet-oxygen quantum yield of 0.43, strong binding affinity towards double-stranded DNA, and thus promising photodynamic activity.

Coordination Chemistry

C. A. Bell, P. V. Bernhardt, L. R. Gahan, M. Martínez, M. J. Monteiro, C. Rodríguez, C. A. Sharrad* .... 3166 – 3175

Copper(II) Complexes of a Hexadentate Mixed-Donor N_3S_3 Macrobicyclic Cage: Facile Rearrangements and Interconversions

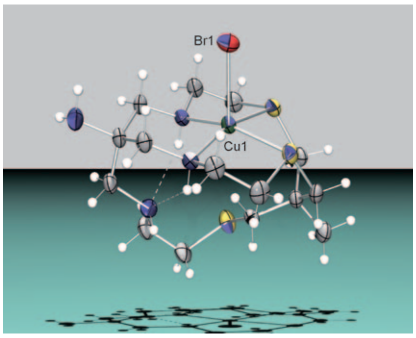

Cage fighter: In contrast to the typically extreme stability and inertness of metal ions trapped within macrobicyclic cage ligands, the six-coordinate Cu^{II} complex of a mixed-donor N_3S_3 cage ligand rapidly rearranges to a bromide complex (see figure) in which the ligand adopts a novel tetradentate coordination mode.

Phase Transitions

*P. Zhu, X. Yan, Y. Su, Y. Yang, J. Li** .... 3176 – 3183

Solvent-Induced Structural Transition of Self-Assembled Dipeptide: From Organogels to Microcrystals

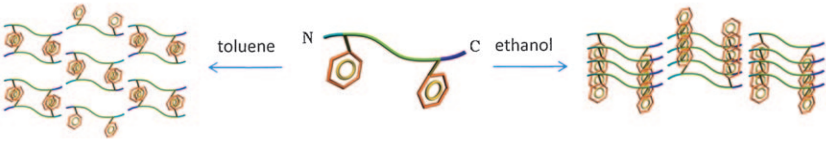

From flexible fibrils to hierarchically self-assembled microcrystals: The structural transition from mesostable dipeptide gels to thermodynamically stable microcrystals is achieved merely by addition of the co-solvent; this provides insights into the role of solvents in controlling molecular arrangements (see scheme).

Donor–Acceptor Systems

C.-H. Chen, Y.-C. Hsu, H.-H. Chou, K. R. J. Thomas, J. T. Lin, C.-P. Hsu* .... 3184 – 3193

Dipolar Compounds Containing Fluorene and a Heteroaromatic Ring as the Conjugating Bridge for High-Performance Dye-Sensitized Solar Cells

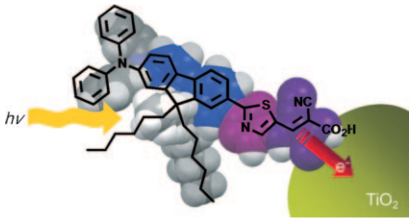

Dipolar organic dyes containing diarylamine as a donor and fluorene and a heteroaromatic ring as the conjugating bridge (see scheme) have been developed for highly efficient nanocrystalline TiO_2 dye-sensitized solar cells (DSSCs). The overall efficiencies of DSSCs range from 4.92–6.88 %, which reach 68–96 % of a standard device of N-719 that was fabricated and measured under the same conditions.

Off the coast: A marine-derived actinomycete, *Nocardiopsis* sp., from a sediment sample collected at the coast of Brisbane, Australia, yielded two new macrolide polyketides, nocardiopsins A (see figure) and B. The nocardiopsins exhibit low-micromolar binding to FKBP12, consistent with their structural and biosynthetic relationship to the immunosuppressive agents FK506 and rapamycin.

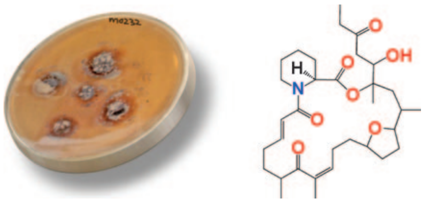

Marine Natural Products

*R. Raju, A. M. Piggott, M. Conte, Z. Tnimov, K. Alexandrov, R. J. Capon** .... 3194 – 3200

Nocardiopsins: New FKBP12-Binding Macrolide Polyketides from an Australian Marine-Derived Actinomycete, *Nocardiopsis* sp.

The wizard of Os: A novel class of highly modular diphosphane/diamine–osmium complexes (see structures) are found to be extremely active catalysts in the hydrogenation of ketones and aldehydes (substrate/catalyst ratios and turnover frequencies of up to 2×10^5 and 3×10^5 h^{-1}, respectively). High enantioselectivity is achieved with the osmium complexes obtained from the new precursor $[Os_2Cl_4\{P(m\text{-tolyl})_3\}_5]$ and the correctly matched chiral ligands.

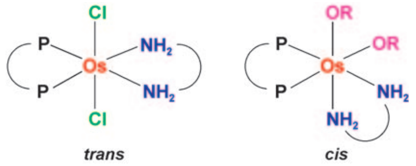

Asymmetric Catalysis

W. Baratta, C. Barbato, S. Magnolia, K. Siega, P. Rigo* .... 3201 – 3206

Chiral and Nonchiral $[OsX_2(\text{diphosphane})(\text{diamine})]$ (X: Cl, OCH_2CF_3) Complexes for Fast Hydrogenation of Carbonyl Compounds

---

Fullerene antioxidants: The mechanism for degradation of the biologically relevant superoxide radical ($O_2^{\bullet-}$) involving the tris-malonyl fullerene compound known as C_3 was investigated in detail by means of DFT calculations (see figure). The capability of C_3 and related fullerenes to remove highly reactive oxygen species is of immediate interest for future applications in the fields of biology and medicine.

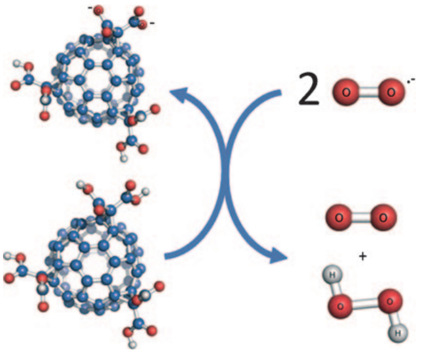

Superoxide Dismutation

S. Osuna, M. Swart, M. Solà** .... 3207 – 3214

On the Mechanism of Action of Fullerene Derivatives in Superoxide Dismutation

---

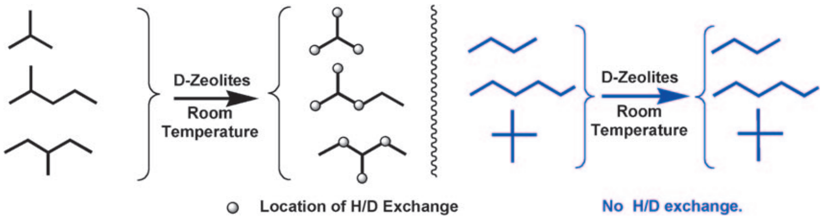

Regioselective H/D exchange occurs between isoalkanes and acidic zeolites at room temperature and it is shown that the main factor controlling the reaction is not the accessibility to the acid sites (see scheme). The deuterium-labeling in various small alkanes is best rationalized by mechanistic schemes typical for classic organic chemistry involving carbocationic intermediates related to the intrinsic reactivity of the alkanes.

Reaction Mechanisms

*A. S. S. Sido, S. Walspurger, J. Barbiche, J. Sommer** .... 3215 – 3221

Room-Temperature Alkane Reactivity in Zeolites: An H/D Exchange Study

Solid-State NMR

J. V. Hanna, K. J. Pike, T. Charpentier, T. F. Kemp, M. E. Smith, B. E. G. Lucier, R. W. Schurko, L. S. Cahill* 3222–3239

A ^{93}Nb Solid-State NMR and Density Functional Theory Study of Four- and Six-Coordinate Niobate Systems

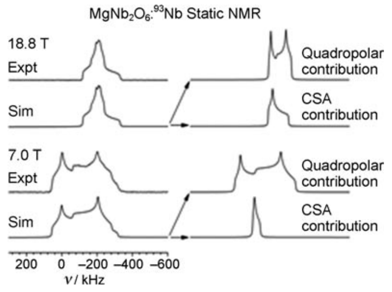

Measurement and calculation: A comprehensive variable B_0 ^{93}Nb broadline solid-state NMR study of a large suite of niobate-based materials is reported. Correlations involving the elucidated ^{93}Nb NMR parameters suggest that the Nb^{V} site is directly influenced by both the immediate oxo environment and the more distant heavy elements comprising the material structure (see figure).

Block Copolymers

S. K. Patra, G. R. Whittell, S. Nagiah, C.-L. Ho, W.-Y. Wong, I. Manners** 3240–3250

Photocontrolled Living Anionic Polymerization of Phosphorus-Bridged [1]Ferrocenophanes: A Route to Well-Defined Polyferrocenylphosphine (PFP) Homopolymers and Block Copolymers

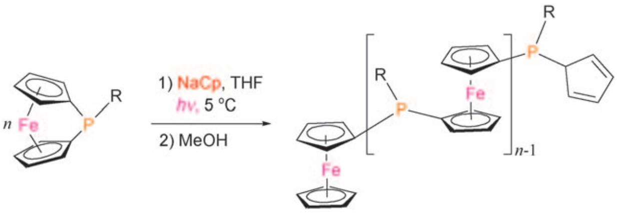

Soft and controlled: Photocontrolled living anionic ring-opening polymerization (ROP) of phosphorus-bridged [1]ferrocenophanes (see scheme) initiated by the mild nucleophile NaCp allows access to well-defined polyferrocenylphosphines with molecular weight control and narrow polydispersities.

* Author to whom correspondence should be addressed

Supporting information on the WWW (see article for access details).

VIP Full Papers labeled with this symbol have been judged by two referees as being "very important papers".

A video clip is available as Supporting Information on the WWW (see article for access details).

SERVICE